

GUALTIERI, C., and CHANSON, H. (2012). "Experimental Study of a Positive Surge. Part 1: Basic Flow Patterns and Wave Attenuation." *Environmental Fluid Mechanics*, Vol. 12, No. 2, pp. 145-159 (DOI 10.1007/s10652-011-9218-z) (ISSN 1567-7419 [Print] 1573-1510 [Online]).

Experimental study of a positive surge. Part 1: Basic flow patterns and wave attenuation

Carlo Gualtieri

Department of Hydraulic, Geotechnical and Environmental Engineering (DIGA), University of Napoli "Federico II", Via Claudio, 21 - 80125, Napoli (Italy) e-mail carlo.gualtieri@unina.it

Hubert Chanson

School of Civil Engineering, The University of Queensland, Brisbane QLD 4072, (Australia) e-mail h.chanson@uq.edu.au

ABSTRACT

A positive surge results from a sudden change in flow that increases the depth. It is the unsteady flow analogy of the stationary hydraulic jump and a geophysical application is the tidal bore. Positive surges are commonly studied using the method of characteristics and the Saint-Venant equations. The paper presents the results from new experimental investigations conducted in a large rectangular channel. Detailed unsteady velocity measurements were performed with a high temporal resolution using acoustic Doppler velocimetry and non-intrusive free-surface measurement devices. Several experiments were conducted with the same initial discharge ($Q=0.060$ m³/s) and 6 different gate openings after closure resulting in both non-breaking undular and breaking bores. The analysis of undular surges revealed wave amplitude attenuation with increasing distance of surge propagation were in agreement with Ippen and Kulin theory. Also, undular wave period and wave length data were relatively close to the values predicted by the wave dispersion theory for gravity waves in intermediate water depths.

KEYWORDS

Environmental hydraulics, positive surge, free surface measurements, instantaneous velocity field, physical modeling, wave attenuation.

1. INTRODUCTION.

Positive surges are commonly observed in man-made and natural channels. In water supply canals for irrigation and water power purposes, a positive surge may be induced by a partial or complete closure of a control structure, e.g. a gate, resulting in a sudden change in flow that increases the water depth [1, 2]. In rivers and estuaries, a form of positive surge is the tidal bore which is a positive surge of tidal origin [3]. Tsunami-induced bores were also observed [3]. Although a positive surge may be analysed using a quasi-steady flow analogy, its inception and development is commonly predicted using the method of characteristics and Saint-Venant equations. After formation, the flow properties immediately upstream and downstream of the surge front must satisfy the continuity and momentum principles [1, 2]. For a fully-developed positive surge, the surge is seen by an observer travelling at the surge speed U as a quasi-steady flow situation called a

hydraulic jump in translation (Fig. 1). In a rectangular, horizontal channel and neglecting friction loss, if the subscripts 0 and *conj* refer, respectively, to the initial flow conditions and conjugate flow conditions, i.e., immediately behind the positive surge front, the solution of the continuity and momentum equations applied to a control volume across the surge front yields:

$$\frac{d_{conj}}{d_0} = \frac{1}{2} \left(\sqrt{1 + 8 Fr^2} - 1 \right) \quad (1)$$

$$\frac{Fr_{conj}}{Fr} = \frac{2^{3/2}}{\left(\sqrt{1 + 8 Fr^2} - 1 \right)^{3/2}} \quad (2)$$

where d_{conj} and d_0 are respectively the new and initial flow depths (Fig. 1), and the Froude numbers Fr and Fr_{conj} are the surge Froude numbers defined respectively as:

$$Fr = \frac{V_0 + U}{\sqrt{g d_0}} \quad (3)$$

$$Fr_{conj} = \frac{V_{conj} + U}{\sqrt{g d_{conj}}}$$

where U is the surge velocity as seen by a stationary observer on the channel bank and positive in the upstream direction and V_0 is the flow velocity (Fig. 1).

Positive surges were studied by hydraulicians and applied mathematicians for a few centuries.

Since Barré de Saint-Venant [4], Boussinesq [5], and Favre [6], several researchers discussed the development of a surge [7, 8, 9, 10, 11, 12, 14]. Classical experimental works on undular surges included Zienkiewicz and Sandover [15], Sandover and Holmes [16], Benet and Cunge [17], and Soares Frazão and Zech [18]. Ponsy and Carbonnell [19] and Treske [20] presented a comprehensive description of surges in trapezoidal channels of large sizes. Most of previous experimental studies were limited to visual observations and sometimes free-surface measurements, but more recently, unsteady turbulence measurements were carried out using particle image velocimetry (PIV) and acoustic Doppler velocimetry (ADV) techniques [21, 22, 25]. Finally, numerical studies of a surge were recently presented [18, 26, 27].

In this paper and its companion, the authors present the results from new experimental works conducted in a large rectangular channel to document the flow field and hydrodynamics

characteristics in positive surges. All experiments were performed with the same initially steady flow rate but for different downstream gate openings after closure. The basic features of the surges and the analysis of wave height attenuation for the undular surges are discussed in this paper. A comparison between previous literature theories and the experimental data for undular surges are presented in the companion paper as well as the results about the unsteady flow field including Reynolds stresses. Overall this study was aimed at confirming and extending previous findings about hydrodynamics characteristics of a positive surge.

2. EXPERIMENTAL SETUP. CHANNEL AND INSTRUMENTATION.

The experiments were performed in a large tilting flume at the University of Queensland previously used by Chanson and co-workers [22, 23, 24, 25]. The channel was 0.5 m wide, 12 m long and it was horizontal. The flume was made of smooth PVC bed and glass walls, and waters were supplied by a constant head tank. The water discharge was measured with orifice meters with an accuracy of less than 2%. A tainter gate was located next to the downstream end, at $x=11.15$ m from the channel intake, where x is the distance from the channel upstream end. Its controlled and rapid closure induced a positive surge propagating upstream.

The study was carried out with a constant flow rate ($Q=0.060$ m³/s). Before the study of the surges, the steady flow in the channel was studied using an acoustic Doppler velocimeter (ADV) Sontek™ 16MHz micro-ADV equipped with a two-dimensional side-looking head. Also, in steady flow, water depths were measured using rail mounted pointer gauges and seven acoustic displacement meters Microsonic™ Mic + 25/IU/TC with an accuracy of 0.18 mm and a response time of 50 ms. The acoustic displacement meters were located at $x=1.985$ m, 2.995 m, 4 m, 5 m, 6 m, 9 m and 10.9 m downstream the channel intake.

After that, several experiments were conducted with the same initial discharge ($Q=0.060$ m³/s) and 6 different gate openings after closure (Table 1). They resulted in both undular (non-breaking) and in breaking surges (Table 1). The unsteady water depths were measured with the above acoustic displacement meters, while the turbulent velocity measurements were conducted with the above ADV system. For both the steady and unsteady state experiments, the velocity range was 1.0 m/s,

the sampling rate was 50 Hz and the data accuracy was 1% of the velocity range. The translation of the ADV probe in the vertical direction was controlled by a fine adjustment travelling mechanism connected to a Mitutoyo™ digimatic scale unit. The error on the vertical position of the probe was $\Delta z < 0.025$ mm. The accuracy on the longitudinal position was $\Delta x < \pm 2$ mm. All measurements were conducted on the channel centreline. Additional information was obtained with digital cameras Panasonic™ Lumix DMC-FZ20GN (shutter: 8 to 1/2,000 s) and Canon™ A85 (shutter: 15 to 1/2,000 s).

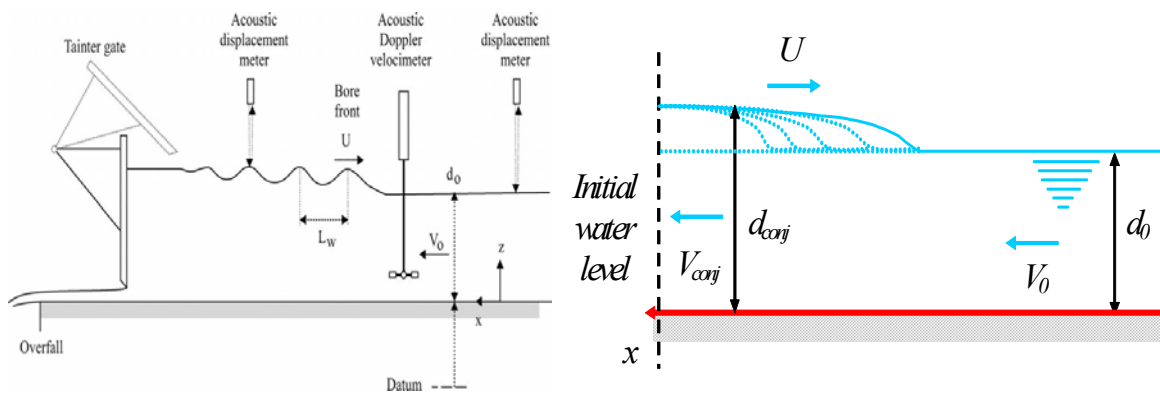


Fig. 1 – Definition sketch of a positive surge. Positive surge for an observer standing on the bank

2.1 ADV METROLOGY.

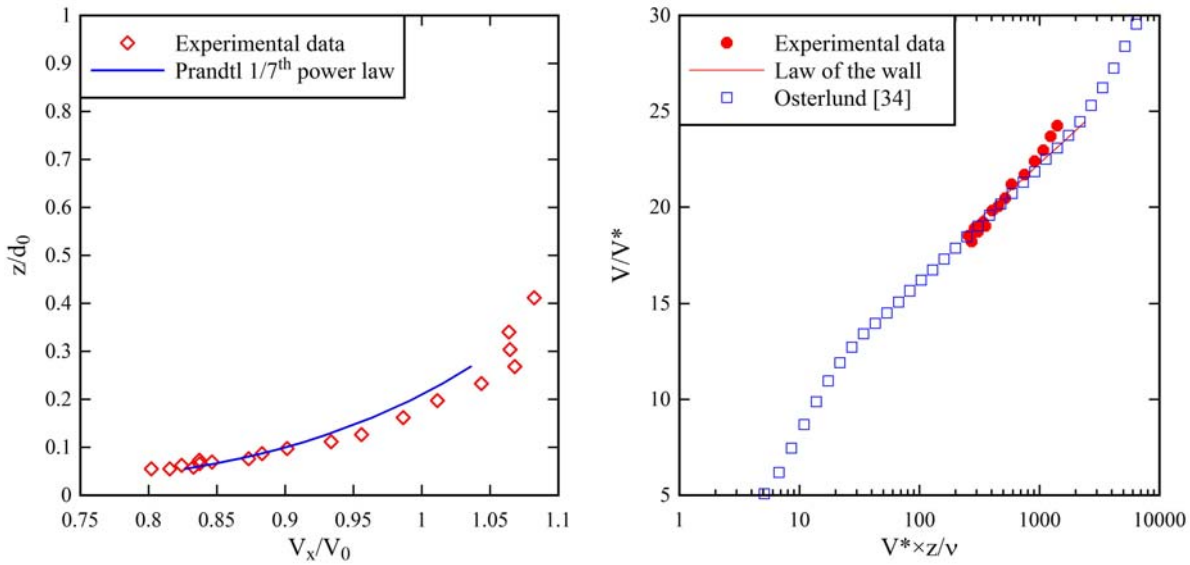
ADV measurements are performed by measuring the velocity of particles in a remote sampling volume based upon the Doppler shift effect [28, 29]. An ADV system records simultaneously four values with each component of a sample: the velocity component, the signal strength value, the correlation value and the signal to noise ratio. Past and present experiences demonstrated many problems because the signal outputs combine the effects of velocity fluctuations, Doppler noise, signal aliasing, turbulent shear and other disturbances [22, 30, 31]. For all experiments, present experience demonstrated recurrent problems with the velocity data, including low correlations and low signal to noise ratios. The situation improved drastically by mixing some vegetable dye (Dytex Dye™ Green) in the entire water recirculation system (Figs. 5–7). The vegetable dye introduced some very fine particles in the water, increasing in turn the number of excited particles in the ADV control volume. The effect of added dye was to increase the time-averaged signal correlations and time-averaged signal to noise-ratios. The buoyancy effect was negligible since the dye particles

were neutrally buoyant.

While several ADV post-processing techniques were devised for steady flows [31, 32], these post-processing techniques are not applicable to unsteady flows [22, 33]. In the present study, unsteady flow post-processing was limited to a removal of communication errors and a replacement by linear interpolation. Note also that spurious data collected by the acoustic displacement meters were removed and the removed points were obtained by linear interpolation of end points. The method is known for the absence of bias.

2.2 STEADY-STATE CONDITIONS

Some detailed measurements of the velocity distributions were performed in the steady flow at $x=5$ m. The results showed that the inflow conditions were partially developed. The boundary layer thickness was about $\delta/d_0=0.265$, where d_0 is the initial flow depth. Note that the thickness of boundary layer was calculated by comparing the experimental data with Prandtl 1/7 power law. This result was close to and consistent with the earlier studies of Koch and Chanson [22] with a lower flow rate and of Chanson [23] with a $Q=0.058$ m³/s and a smooth bed, where δ/d_0 was 0.32. Fig. 2 presents the dimensionless vertical velocity profile on the channel centreline ($y/W = 0.5$), where W is the channel width. In the boundary layer, the longitudinal velocity profile favorably compared to a 1/7th power law. The boundary layer characteristics were calculated. The velocity data were in agreement with theoretical velocity profiles in turbulent boundary layer and to some experimental data collected by Osterlund [34] in a large wind tunnel operating at comparable Reynolds numbers (Fig. 3). From the data best fit with the low law, the shear velocity was estimated: $V^*=0.0375$ m/s close to the finding of Koch and Chanson [22] for a lower discharge. The findings demonstrated that the flume was *hydraulically smooth* and the flow was smooth turbulent.



Figs. 2–3 – Dimensionless velocity distributions in the initially steady flow. Time-averaged velocities V_x/V_0 – Comparison between ADV data and 1/7th power law. (left) and between ADV data, law of the wall and Osterlund [34] (right)

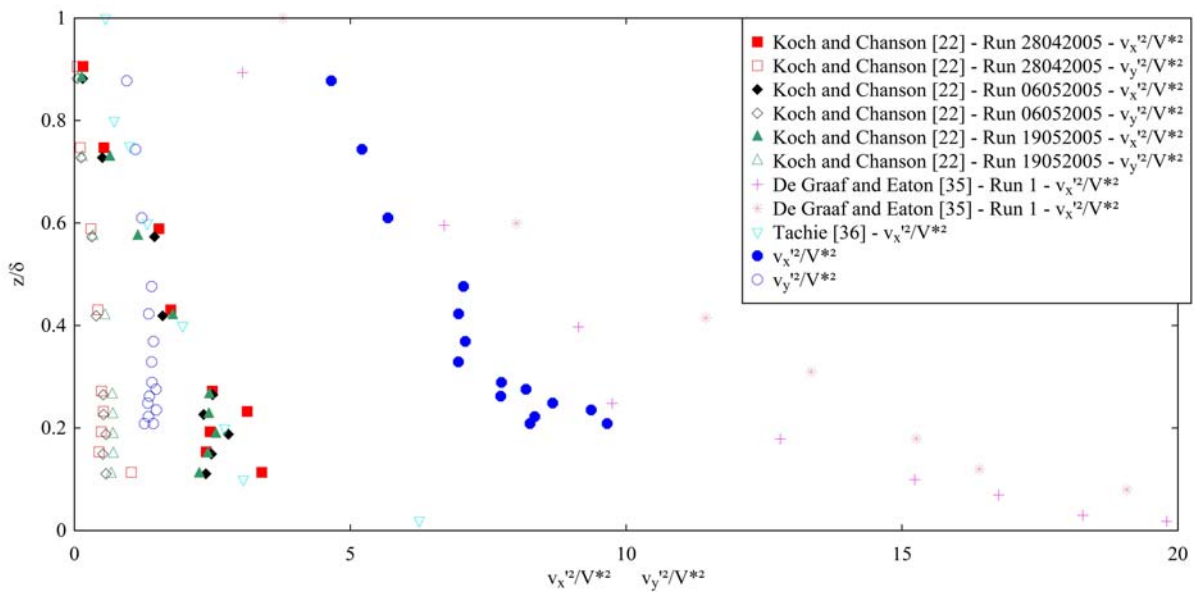


Fig. 4 – Dimensionless distributions of normal Reynolds stresses $v'_x{}^2/V^{*2}$ and $v'_y{}^2/V^{*2}$ in the initially steady flow. Comparison with the data of Koch and Chanson [22], De Graaf and Eaton [35] and Tachie [36]

Fig. 4 presents the dimensionless distributions of normal Reynolds stresses $v'_x{}^2/V^{*2}$ and $v'_y{}^2/V^{*2}$ as

functions of z/δ on channel centerline. The ratio $v'_y{}^2/v'_x{}^2$ was in average about 0.32, which is close to the previous results, e.g. 0.28 from Koch and Chanson [22] and 0.24 from Chanson [23] (Table 2). The data showed further a good qualitative agreement with the detailed experiments of De Graaf and Eaton [35] in a large wind tunnel and Tachie [36] in smooth open channel flows.

2.3 POSITIVE SURGE GENERATION

The study of positive surges was conducted with one set of initial flow conditions (Table 1). The experimental setup was selected to generate both undular (non-breaking) and breaking (weak) surges with the same initial conditions. The initial flow conditions were supercritical (Eq. (3)). The only dependant parameter was the downstream gate opening after closure. Steady gradually-varied flow conditions were established for at least 5 min prior to measurements and the flow measurements data acquisition was started about 1.5 min prior to gate closure. A positive surge was generated by the rapid partial closure of the downstream gate. The gate closure time was less than 0.2 s [22, 26]. After closure the surge propagated upstream and each experiment was stopped when the bore front reached the intake structure.

Six gate openings after closure were tested (Table 1). In Table 1, h_g is the gate opening and the surge front celerity U was calculated using the displacement meters data between $x=6$ m and 4 m; also, d_0 was measured at $x=5$ m and d_{conj} was derived using Eq. (1). Lastly in Table 1 the data for Run 60-1, 60-6 and Run 60-7 refer to the average of 23 runs with the same gate opening but different vertical elevation z for the ADV system sampling volume.

The free-surfaces were studied using seven displacement meters. For three cases, detailed velocity measurements were also performed using the ADV system located at a distance $x=5$ m downstream of the channel intake and on the channel centerline. The earlier work of Koch and Chanson [22] showed little transverse differences but close to the sidewall where the ADV system was further adversely affected by the sidewall proximity. Note that, if the structure of flow in positive surges is generally 3D, previous studies showed a quasi-2D free-surface in breaking, weak surges [22].

The experimental results were compared to previous literature data, whose flow conditions are listed in Table 2. Note that flume and channel experiments refer to laboratory and field experiments

respectively.

Table 1 – Experimental flow conditions

Run	Q – m ³ /s	d ₀ – m	h _g – m	Type	U – m/s	d _{conj} – m	Fr	Remarks
60-1	0.060	0.1387	0.050	Undular	0.777	0.215	1.408	No ADV
60-1	0.060	0.1447	0.050	Undular	0.753	0.209	1.328	ADV measurements
60-2	0.060	0.1396	0.040	Undular	0.857	0.228	1.466	No ADV
60-3	0.060	0.1396	0.025	Undular	0.875	0.231	1.483	No ADV
60-5	0.060	0.1403	0.010	Weak	0.946	0.242	1.536	No ADV
60-6	0.060	0.1369	0.005	Weak	0.911	0.238	1.543	No ADV
60-6	0.060	0.1429	0.005	Weak	0.918	0.237	1.484	ADV measurements
60-7	0.060	0.1427	0.100	Undular	0.519	0.171	1.149	ADV measurements

Table 2 – Previous experimental investigations on positive surges

References	Q – m ³ /s	d ₀ – m	h _g – m	Type	U – m/s	d _{conj} – m	Fr	Remarks
Favre [6]	---	0.106 to 0.265	---	Undular	---	---	1.05 to 1.21	Flume exp.
Benet and Cunge [17]	0.002 to 0.006	0.057 to 0.150	---	Undular & Weak	---	---	1.05 to 1.33	Flume exp.
Benet and Cunge [17]	13 to 235	6.61 to 9.21	---	Undular & Weak	---	---	1.06 to 1.16	Channel exp.
Benet and Cunge [17]	270 to 300	5.62 to 7.53	---	Undular & Weak	---	---	1.06 to 1.16	Channel exp.
Treske [20]	0.04 to 0.16	---	---	Undular	---	---	1.04 to 1.38	Flume exp.
Koch and Chanson [22]	0.040	0.0785 to 0.0795	0.010 to 0.092	Undular & Weak	0.140 to 0.682	0.096 to 0.156	1.31 to 1.92	Flume exp.
Chanson [23]	0.058	0.1385	0.100	Undular	0.553	0.169	1.17	Flume exp. – 2 type of bed roughness
Chanson [24]	0.019 to 0.051	0.101 to 0.205	0.009 to 0.061	Undular & Weak	0.680 to 1.316	0.209 to 0.404	1.09 to 1.95	Flume exp.

2.4 REYNOLDS STRESS ESTIMATES IN RAPIDLY-VARIED FLOW MOTION

In turbulence studies, the measured statistics are based upon the analysis of instantaneous turbulent velocity data:

$$v = V - \bar{V} \quad (4)$$

where \bar{V} is a time-average velocity. If the flow is *gradually varied*, \bar{V} must be a low-pass filtered velocity component, or variable-interval time average VITA [37, 38]. This technique is based upon a Fourier decomposition and was previously applied to a positive surge [22, 23, 38]. The cutoff frequency must be selected such that the averaging time is greater than the characteristic period of

fluctuations, and small with respect to the characteristic period for the time-evolution of the mean properties [39]. In highly unsteady flows, experiments have to be repeated many times, and the turbulent velocity fluctuation becomes the deviation of the instantaneous velocity from the ensemble average [22, 38].

In undular surge flows, the Eulerian flow properties showed an oscillating pattern with a period of ranging from 1.01 to 1.87 s that corresponded to the period of the free-surface undulations. The unsteady data were therefore filtered with a low/high-pass filter threshold greater than 0.99 Hz (i.e. $1/1.01$ s) and smaller than the Nyquist frequency (herein 25 Hz). The cutoff frequency was selected as 1 Hz based upon previous experiences [22, 23]. The same filtering technique was applied to both longitudinal and transverse velocity components, and for both weak and undular surge experiments. The Reynolds stresses were calculated from the high-pass filtered signals.

3. BASIC FLOW PATTERNS.

Non-intrusive unsteady free-surface measurements were performed for a range of partial gate closures (Table 1). For large gate openings, the surge propagation was relatively slow and the bore front was followed by a train of well-formed undulations: this is typical of an *undular surge*. At the lowest Froude number, i.e. $Fr=1.15$ (Run 60-7), the free-surface undulations had a *smooth* appearance and no wave breaking and no formed roller was observed (Fig. 5).

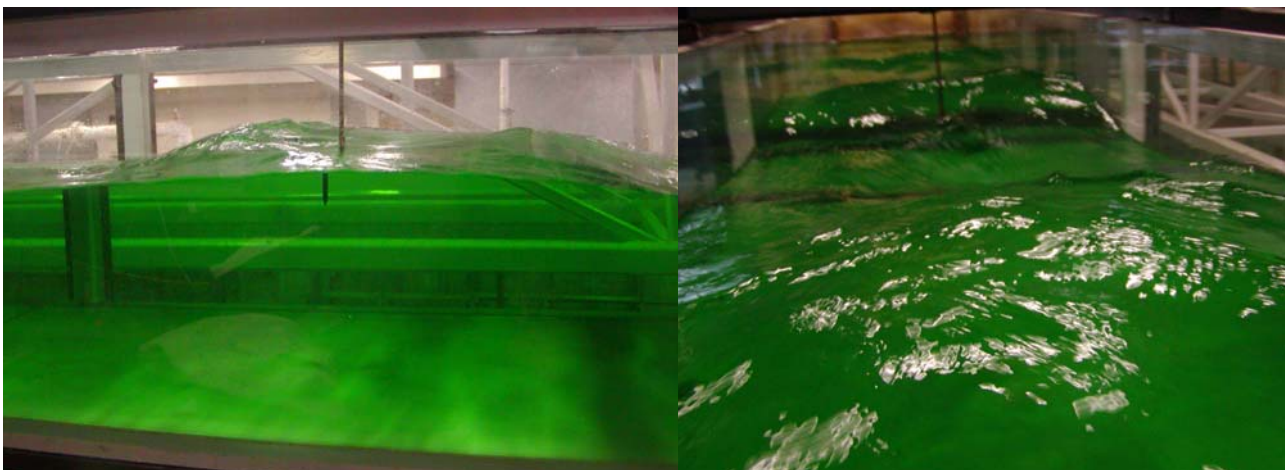


Fig. 5 – Undular surge, Run 60-7. Lateral view (left) and looking downstream at the incoming first wave crest (right)

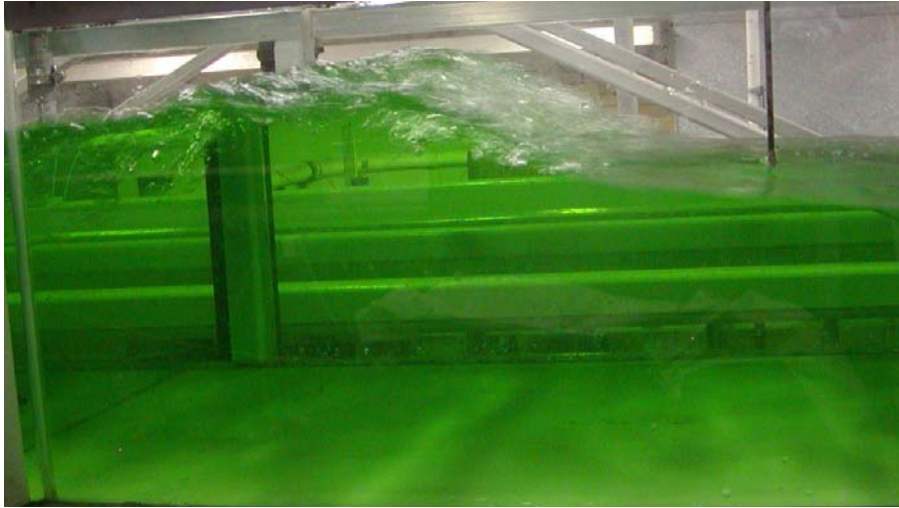


Fig. 6 – Undular surge with some breaking, Run 60-1. Lateral view (above) and looking downstream at the incoming wave crest (below)



However some cross-waves, or sidewall shock waves, were seen developing upstream of the propagation of the first wave crest and intersecting next to the first crest. The cross-waves propagated behind the first wave crest, they were reflected on the opposite sidewall and they gave a lozenge pattern to the free-surface. A similar cross-wave pattern was observed in stationary undular hydraulic jumps [40, 41] and undular surges [22, 23].

For intermediate-surge Froude numbers, in the range from 1.3 to 1.45–1.5, some wave breaking was observed at the bore front and the ensuing free surface undulations were flatter (Fig. 6). The surge front celerity was greater than that of non-breaking undular surges (Table 1, column 6).

For $Fr > 1.5$, breaking (weak) surges were observed (Fig. 7). They propagated at a relatively faster speed, and the free-surface appeared to be quasi-two-dimensional, whereas previous studies demonstrated that undular surges have a three-dimensional flow structure [22]. Also, the bore front

was associated with some air entrainment in the roller (Fig. 7).

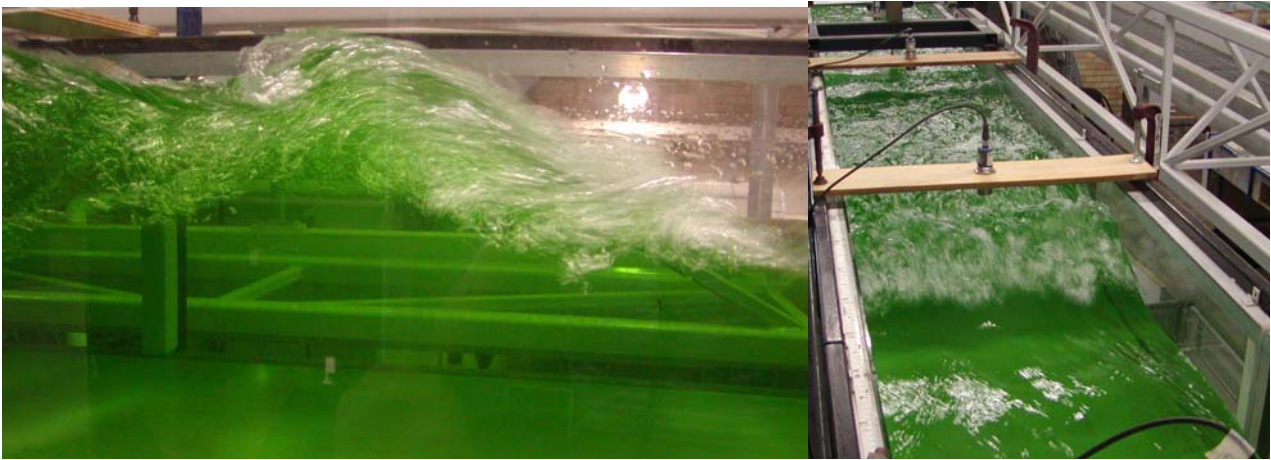


Fig. 7 – Breaking surge, Run 60-6. Lateral view (left) and looking downstream at the incoming wave crest (right)

For the entire range of investigations, the bore celerity ranged from 0.52 to 0.95 m/s (Table 1, column 6), while the wave period was 1.87 s and 1.01 s as seen by an observer fixed on the bank for Run 60-7 and Run 60-1 respectively. Overall the flow patterns were consistent with earlier studies [6, 20, 22, 23].

Typical instantaneous free-surface profiles are presented in Figs. 8, 9 and 10. Each curve shows the instantaneous dimensionless flow depth d/d_0 as a function of the dimensionless time from gate closure $t \times (g/d_0)^{0.5}$. Note that the zero dimensionless time corresponded to 10.0 seconds prior to the first wave crest passage at the sampling location. Fig. 8 presents data for the undular surge (Run 60-7) at two locations, i.e. $x=6$ m and $x=5$ m. The free-surface data showed a slight evolution of the positive surge shape as it propagated upstream. It is conceivable that the bore was not fully developed. However, the data tended to suggest a gentle reduction of the bore height with increasing distance from the downstream gate. This trend was consistent with a fully developed bore propagating against a non uniform gradually varied flow and with previous findings [22]. Also a general asymmetry of undulations was noted as discussed by Chanson [24].

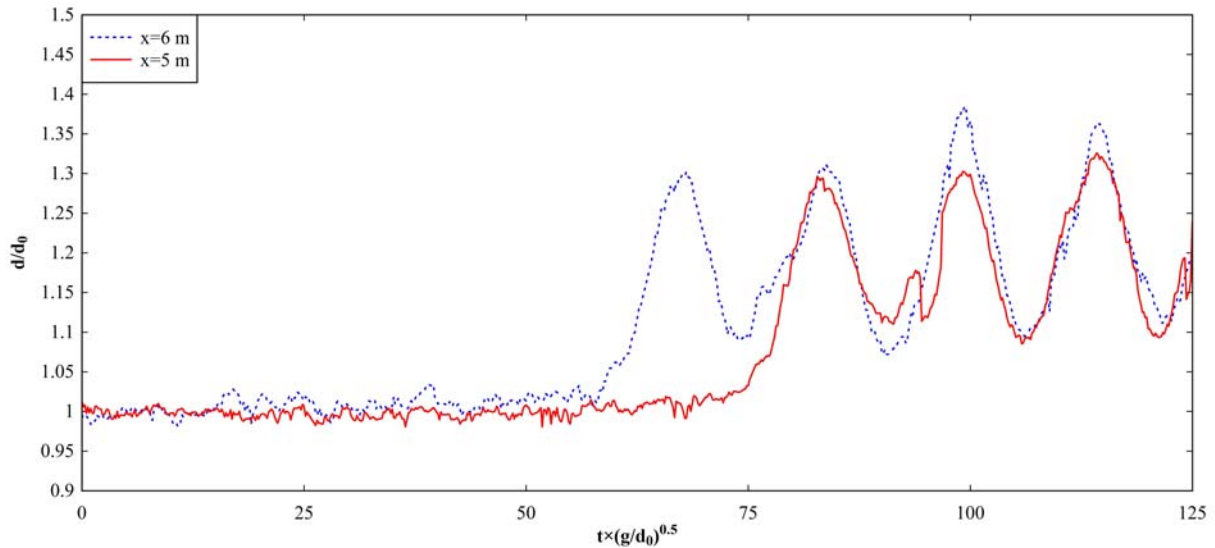


Fig. 8 – Undular surge, Run 60-7. Dimensionless instantaneous water depth d/d_0

Fig. 9 presents the instantaneous free-surface profile for the undular surge with some breaking (Run 60-1) at two locations, i.e. $x=6$ m and $x=5$ m. It could be noted that the period of surface undulations was smaller than for Run 60-7.

Finally, Fig. 10 shows data for the weak surge (Run 60-6) at $x=6$ m and $x=5$ m. The roller passage was associated with a marked discontinuity of the free-surface, although the free-surface elevation rose slowly immediately prior to the roller, with the free-surface curving upwards ahead of the roller toe [22]. The maximum water depth was very similar in the two locations

The free-surface profiles at $x=5$ m were not significantly affected by the vertical elevation of the ADV system. In a fully-developed surge, the ratio of conjugate depths (d_{conj}/d_0) must satisfy the continuity and momentum equations (Eq. (1)). Present experimental results were generally close to those predicted by the momentum principle, although some undular surge data gave lower conjugate depth ratios.

Both in Figs. 8, 9 and 10, some spurious points and missing data could be noted. The acoustic displacement meter output was a function of the strength of the acoustic signal reflected by the free-surface. When the free-surface was not horizontal, some erroneous points were recorded. These were relatively isolated and easily ignored.

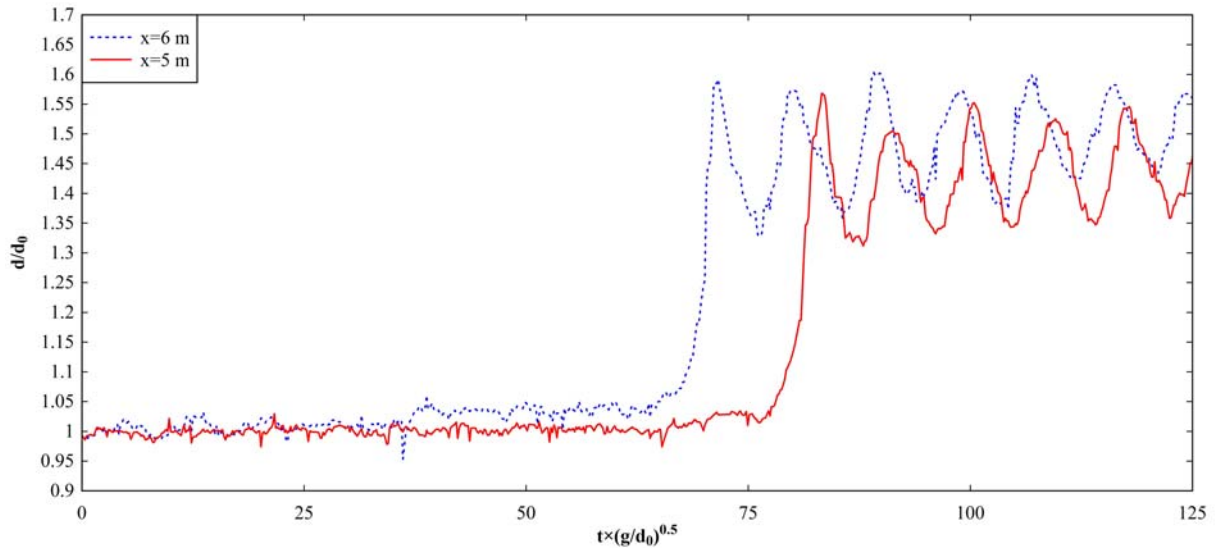


Fig. 9 – Undular surge with some breaking, Run 60-1. Dimensionless instantaneous water depth d/d_0

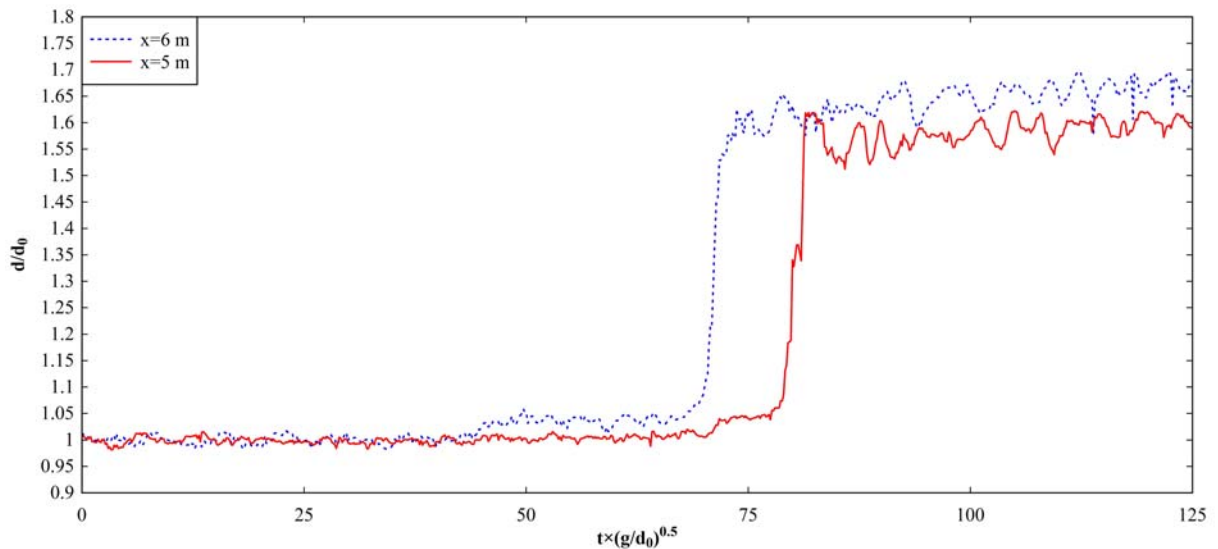


Fig. 10 – Breaking surge, Run 60-6. Dimensionless instantaneous water depth d/d_0

4. UNDULAR SURGES. FREE-SURFACE PROPERTIES. WAVE HEIGHT ATTENUATION

A key feature of undular surges is the secondary wave motion illustrated in Figs. 8–9 with the dimensionless time variations in the water depth at several longitudinal distances for $Fr=1.15$ and 1.35 . In surges and hydraulic jumps, the equation of conservation of momentum may be applied across the jump front together with the equation of conservation of mass [1, 2]. When the rate of

energy dissipation is negligible as in an undular surge, there is a quasi-conservation of energy. Let us follow the surge in the system of coordinates in translation with the undular surge front. The equations of conservation of momentum and energy can be rewritten as [24]:

$$\frac{M}{d_c^2} = \frac{d_c}{d} + \frac{1}{2} \left(\frac{d}{d_c} \right)^2 = \text{const} \quad (5)$$

$$\frac{E}{d_c} = \frac{d}{d_c} + \frac{1}{2} \left(\frac{d_c}{d} \right)^2 = \text{const} \quad (6)$$

where M is the momentum function, E is similar to the energy per unit mass, also called the specific energy, and d is flow depth. For a surge in a rectangular channel, d_c equals:

$$d_c = \sqrt[3]{\frac{[(V_0 + U)d_0]^2}{g}} \quad (7)$$

Note that Eq. 5 is always valid but Eq. 6 is an approximation only applicable to an undular surge with a small Froude number close to unity. In this case, Eqs. (5) and (6) may be considered as a parametric representation of the relationship between the dimensionless momentum M/d_c^2 and energy E/d_c [9, 24]. The function $M-E$ has two branches intersecting at $M/d_c^2=1.5$ and $E/d_c=1.5$ (Fig. 11, left). The branches represent the only possible relationship between M/d_c^2 and E/d_c in a surge if both Eqs. (5) and (6) hold. The right branch of the curve $M-E$ corresponds to the supercritical flow while the upper branch (or left branch) corresponds to a subcritical flow.

Fig. 11, right, presents a comparison between Eqs. 5–6 and some experimental data for Run 60-7 and Run 60-1. The graph includes the initial flow conditions and the undular flow data between the first and fourth wave crests. The data justified the approximation of negligible energy losses, i.e. Eq. (6), because all the data were located on the parametric curve $M-E$. The finding was consistent with [24]. Furthermore the undular flow data was on the subcritical flow branch of the $M-E$ curve. Also, there is a greater momentum function and specific energy at the first wave crest than in the initial flow (blue empty square and red empty circle). This was because Eqs. (5) and (6) are based on the assumption of hydrostatic pressure distribution, but the free-surface curvature at the wave crest implies a pressure gradient less than hydrostatic, hence a smaller specific energy.

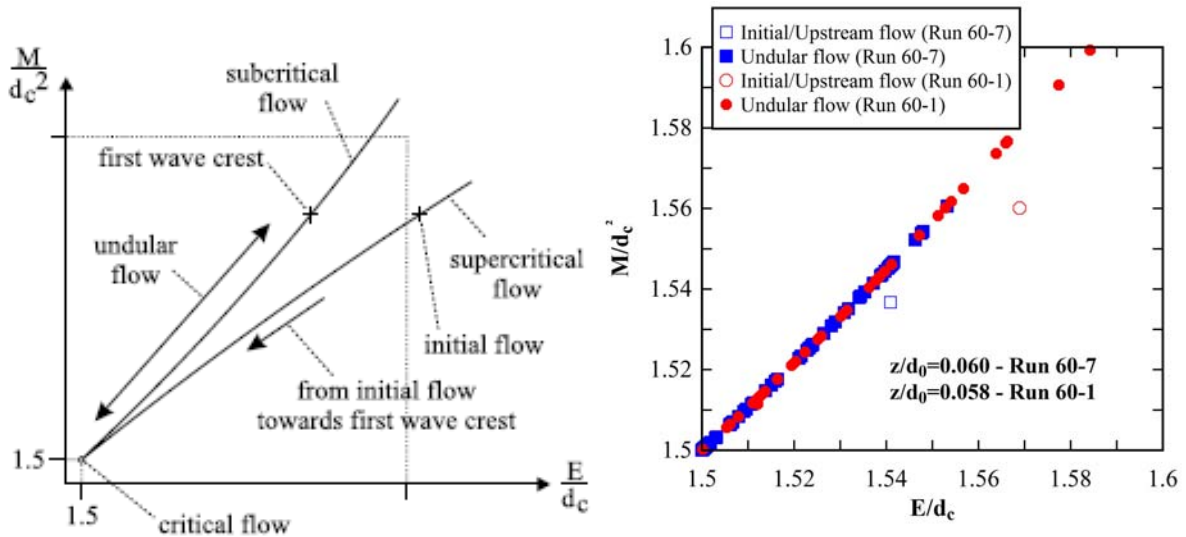


Fig. 11 – Dimensionless relationship between momentum and energy fluxes in undular surges.

Definition sketch after [24] (left) and experimental data for Run 60-7 and Run 60-1 (right)

For sinusoidal water waves, Ippen and Kulin [42] developed an estimate for the wave amplitude attenuation due to boundary friction as:

$$\frac{\Delta d/d}{(\Delta d/d)_{x=x_0}} = \left(1 + \frac{2}{15} f \frac{(x_0 - x)/d}{\Delta d/d} \right) \quad (8)$$

where Δd is the attenuated positive wave height at a distance $(x_0 - x)$ from the reference location x_0 , where the wave height is $\Delta d_{x=x_0}$, d is water depth measured at x , and f is Darcy-Weisbach friction factor. The undular surge propagation data showed some attenuation of the wave height Δd with increasing distance of bore propagation as previously shown by [23].

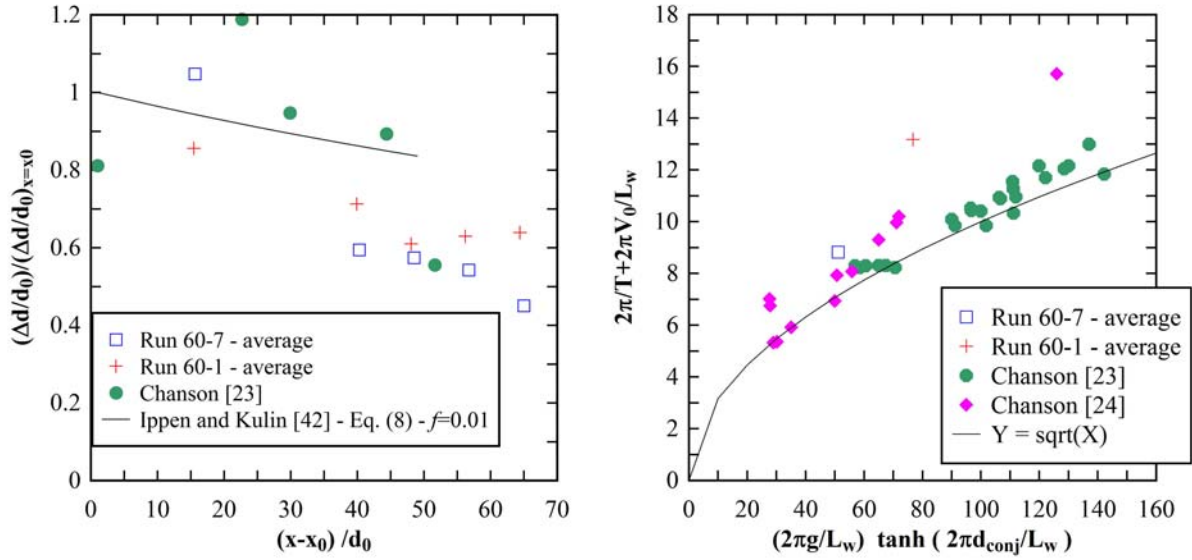


Fig. 12 – Undular surges. Wave height attenuation (left) and wave dispersion (right)

Fig. 12, left, presents the averaged data for Run 60-7 and Run 60-1, which are compared to Eq. (8) assuming $f = 0.01$ [23], and to previous data for smooth bed, $Q=0.058 \text{ m}^3/\text{s}$ and $Fr=1.17$ [23]. The experimental data were in agreement with the previous literature data [23, 42], whereas for larger $(x-x_0)/d_0$ they were below Eq. (8). Moreover, the attenuation was lower for the undular surge with some breaking (Run 60-1). This was expected since for this surge the wave height was quite similar at different measurement points (Fig. 9). Note finally that Eq. (8) holds strictly only for an undular surge.

The undular wave period and wavelength data were further compared to the wave dispersion theory for gravity waves in intermediate water depths. For a wave propagating upstream in presence of a current with an initial velocity V positive downstream, the linear wave theory yields a dispersion relationship between the angular frequency $2\pi/T$ and wave number $2\pi/L_w$:

$$\frac{2\pi}{T} + \frac{2\pi V}{L_w} = \sqrt{\frac{2\pi g}{L_w} \tanh\left(\frac{2\pi d}{L_w}\right)} \quad (9)$$

where L_w is wavelength and d is the initially still water depth [43, 44]. For the free-surface undulations of an undular surge propagating against a current with an initial velocity V_0 , Eq. (9) becomes:

$$\frac{2\pi}{T} + \frac{2\pi V_0}{L_w} = \sqrt{\frac{2\pi g}{L_w} \tanh\left(\frac{2\pi d_{conj}}{L_w}\right)} \quad (10)$$

In Fig. 12, right, Eq. (10) is compared to averaged experimental data from Run 60-7 and Run 60-1 and with previous literature data [23, 24]. The averaged data from Run 60-7 was in good agreement with previous data, as well as with Eq. (10), but the averaged data from Run 60-1, where some breaking was observed, was quite above Eq. (10). However it must be stressed that Eq. (10) was developed for regular waves rather than for the undular bore secondary waves.

5. CONCLUSION.

New experiments of positive surges were conducted under controlled flow conditions in a large channel. Detailed turbulence measurements were performed with a high-temporal resolution (50 Hz) using side looking acoustic Doppler velocimetry and non-intrusive free surface measurement devices. Using the same initially steady flow conditions, several experiments were performed in non-breaking and breaking surges propagating upstream against the initial flow. The dependant variable was the downstream gate opening after closure.

Both undular and breaking surges were observed. At the lowest surge Froude numbers, i.e. $Fr=1.15$, the bore was an undular surge. The wave front was followed by a train of well-formed free surface undulations. Some breaking was seen at the first wave crest for Fr in the range from 1.3 to 1.5. For larger surge Froude numbers, i.e. $Fr > 1.7$, a weak breaking surge was observed. The range of Froude numbers corresponding to each type of surge was consistent with the literature findings [22, 23]. Furthermore, a detailed analysis of undular surges characteristics was carried out. First, the experimental results matched the $M-E$ function proposed by Benjamin and Lighthill [9], implying that the rate of energy dissipation was small to negligible. Second, the experimental data for wave amplitude attenuation with increasing distance of surge propagation were in agreement with Ippen and Kulin theory [42]. Third, the undular wave period and wave length data were relatively close to the values predicted by the wave dispersion theory for gravity waves in intermediate water depths [43].

In a companion paper [45], a comparison between previous literature theories and the experimental data for undular surges as well as the results about the unsteady flow field including Reynolds

stresses will be presented.

REFERENCES.

- [1] Henderson, F.M. (1966). Open channel flow. MacMillan Company, New York, USA.
- [2] Chanson, H. (2004a). The hydraulics of open channel flows: An introduction. Butterworth-Heinemann, Oxford, UK, 2nd edn, 630.
- [3] Chanson, H. (2011). Current knowledge in tidal bores and their environmental, ecological and cultural impacts. *Environmental Fluid Mechanics*, Vol. 11, No. 1, pp. 77-98 (DOI: 10.1007/s10652-009-9160-5).
- [4] Barré de Saint-Venant, A.J.C. (1871). Théorie et equations générales du mouvement non permanent des eaux courantes. *Comptes Rendus des séances de l'Académie des Sciences, Paris, France*, Séance 17 July 1871, 73, 147–154 (in French).
- [5] Boussinesq, J.V. (1877). Essai sur la théorie des eaux courantes.(Essay on the Theory of Water Flow). *Mémoires presents par divers savants à l'Académie des Sciences, Paris, France*, Vol. 23, Série 3, No. 1, supplément 24, 1–680 (in French).
- [6] Favre, H. (1935). Etude théorique et expérimentale des ondes de translation dans les canaux découverts (Theoretical and Experimental Study of Travelling Surges in Open Channels). Dunod, Paris, France (in French).
- [7] Lemoine, R. (1948). Sur les ondes positives de translation dans les canaux et sur le ressaut ondulé de faible amplitude (On the Positive Surges in Channels and on the Undular Jumps of Low Wave Height). *La Houille Blanche*, Mar–Apr., 183–185 (in French).
- [8] Serre, F. (1953). Contribution à l'étude des écoulements permanents et variables dans les canaux (Contribution to the Study of Permanent and Non-Permanent Flows in Channels). *La Houille Blanche*, 830–872 (in French).
- [9] Benjamin, T.B., Lighthill, M.J. (1954). On cnoidal waves and bores. *Proc. Royal Soc. of London, Series A, Math. & Phys.Sci.* 224(1159), 448–460.
- [10] Peregrine, D.H. (1966). Calculations of the development of an undular bore. *J. Fluid Mech.* 25, 321–330.

GUALTIERI, C., and CHANSON, H. (2012). "Experimental Study of a Positive Surge. Part 1: Basic Flow Patterns and Wave Attenuation." *Environmental Fluid Mechanics*, Vol. 12, No. 2, pp. 145-159 (DOI 10.1007/s10652-011-9218-z) (ISSN 1567-7419 [Print] 1573-1510 [Online]).

- [11] Wilkinson, D.L., Banner, M.L. (1977). Undular bores. Proceeding of 6th Australasian Hydraulic and Fluid Mechanics Conference, Adelaide, Australia, 369–373.
- [12] Teles da Silva, A.F., Peregrine, D.H. (1990). Non steady computations of undular and breaking bores. Proceeding of the 22nd International Congress Coastal Engineering, Delft, The Netherlands, ASCE Publ., 1, 1019–1032.
- [13] Sander, J., Hutter, K. (1991). On the development of the theory of the solitary wave. A historical essay. *Acta Mechanica* 86, 111–152.
- [14] Sobey, R.J., Dingemans, M.W. (1992). Rapidly varied flow analysis of undular bore. *J. Waterway, Port, Coastal and Ocean Engrg.*, ASCE 118(4), 417–436.
- [15] Zienkiewicz, O.C., Sandover, J.A. (1957). The undular surge wave. Proceeding of the 7th IAHR Congress, Vol. II, Lisbon, Portugal, paper D25, D1–11.
- [16] Sandover, J.A., Holmes, P. (1962). The hydraulic jump in trapezoidal channels. *Water Power* 14, 445–449.
- [17] Benet, F., Cunge, J.A. (1971). Analysis of experiments on secondary undulations caused by surge waves in trapezoidal channels. *J. Hydraul. Res. IAHR* 9(1), 11–33.
- [18] Soares Frazão, S., Zech, Y., (2002). Undular bores and secondary waves — experiments and hybrid finite-volume modelling. *J. Hydraul. Res., IAHR* 40(1), 33–43.
- [19] Ponsy, J., Carbonnell, M. (1966). Etude Photogrammétrique d'Intumescences dans le Canal de l'Usine d'Oraison (Basses-Alpes) (Photogrammetric Study of Positive Surges in the Oraison Powerplant Canal). *J. Soc. Française de Photogram* 22, 18–28 (in French).
- [20] Treske, A. (1994). Undular bores (Favre-waves) in open channels — Experimental studies. *J. Hydraul. Res., IAHR* 32(3), 355–370. Discussion: 33(3), 274–278.
- [21] Hornung, H.G., Willert, C., Turner, S. (1995). The flow field downstream of a hydraulic jump. *J. Fluid Mech.* 287, 299–316.
- [22] Koch, C., Chanson, H. (2009). Turbulence measurements in positive surges and bores. *J. Hydraul. Res.*, 47(1), 29–40.
- [23] Chanson, H. (2010). Unsteady turbulence in tidal bores: Effects of bed roughness. *J. Waterway, Port, Coastal, and Ocean Engineering* 136(5), 247–256.

GUALTIERI, C., and CHANSON, H. (2012). "Experimental Study of a Positive Surge. Part 1: Basic Flow Patterns and Wave Attenuation." *Environmental Fluid Mechanics*, Vol. 12, No. 2, pp. 145-159 (DOI 10.1007/s10652-011-9218-z) (ISSN 1567-7419 [Print] 1573-1510 [Online]).

- [24] Chanson, H. (2010). Undular Tidal Bores: Basic Theory and Free-Surface Characteristics. *J. Hydraul. Engrg.*, ASCE 136(11), 940–944.
- [25] Chanson, H., Tan, K.K. (2010) Turbulent mixing of particles under tidal bores: an experimental analysis, *Journal of Hydraulic Research*, 48(5), 641–649.
- [26] Lubin, P., Chanson, H., Glockner, S. (2010). Large Eddy Simulation of Turbulence Generated by a Weak Breaking Tidal Bore. *Environmental Fluid Mechanics*, Vol. 10, No. 5, pp. 587-602.
- [27] Furuyama, S., and Chanson, H. (2008). A Numerical Solution of a Tidal Bore Flow. *Coastal Engineering Journal*, Vol. 52, No. 3, 215–234.
- [28] Voulgaris, G., Trowbridge, J.H. (1998). Evaluation of the acoustic Doppler Velocimeter (ADV) for turbulence measurements. *J. Atmosph. Oceanic Tech.* 15, 272–289.
- [29] McLelland, S.J., Nicholas, A.P. (2000). A new method for evaluating errors in high-frequency ADV measurements. *Hydrological Processes* 14, 351–366.
- [30] Lemmin, U., Lhermitte, R. (1999). ADV measurements of turbulence: Can we improve their interpretation? Discussion. *J. Hydraul Engrg.*, ASCE 125(6), 987–988.
- [31] Goring, D.G., Nikora, V.I. (2002). Despiking acoustic Doppler velocimeter data. *J. Hydraul. Engrg.*, ASCE 128(1), 117–126. Discussion: 129(6), 484–489.
- [32] Wahl, T.L. (2003). Despiking acoustic Doppler Velocimeter data. Discussion. *J. Hydraul. Engrg.*, ASCE 129(6), 484–487.
- [33] Nikora, V. (2004). Person. Comm., July, Gold Coast, Australia.
- [34] Osterlund, J.M. (1999). Experimental Studies of Zero Pressure-Gradient Turbulent Boundary Layer Flow. Ph.D. thesis, Dept of Mechanics, Royal Institute of Technology, Stockholm, Sweden. Databank: {<http://www2.mech.kth.se/~jens/zpg/index.html>}.
- [35] De Graaf, D.B., Eaton, J.K. (2000). Reynolds-Number Scaling of the Flat-Plate Turbulent Boundary Layer. *Jl of Fluid Mech.*, Vol. 422, pp. 319-346.
- [36] Tachie, M.F. (2001). Open channel turbulent boundary layers and wall jets on rough surfaces. Ph.D. Thesis, Dept. of Mech. Eng., Univers. of Saskatchewan, Canada, 238.
- [37] Piquet, J. (1999). *Turbulent Flows. Models and Physics*. Springer, Berlin, Germany, 761.
- [38] Chanson, H., Docherty, N.J. (2010). Unsteady Turbulence in Tidal Bores: Ensemble-Average or VITA? *Proc. 17th Australasian Fluid Mechanics Conference*, Auckland, New Zealand, 5-9 Dec.,

GUALTIERI, C., and CHANSON, H. (2012). "Experimental Study of a Positive Surge. Part 1: Basic Flow Patterns and Wave Attenuation." *Environmental Fluid Mechanics*, Vol. 12, No. 2, pp. 145-159 (DOI 10.1007/s10652-011-9218-z) (ISSN 1567-7419 [Print] 1573-1510 [Online]).

G.D. Mallinson and J.E. Cater Eds., Paper 034, 4 pages (ISBN: 978-0-86869-129-9).

[39] Bradshaw, P. (1971). An introduction to turbulence and its measurement. Pergamon Press, Oxford, UK, The Commonwealth and International Library of Science and Technology Engineering and Liberal Studies, Thermodynamics and Fluid Mechanics Division, 218.

[40] Chanson, H., Montes, J.S. (1995). Characteristics of undular hydraulic jumps. Experimental apparatus and flow patterns. *J.Hydraul. Engrg.*, ASCE 121(2), 129–144. Discussion: 123(2), 161–164.

[41] Ohtsu, I., Yasuda, Y., Gotoh, H. (2001). Hydraulic condition for undular-jump formations. *J Hydraul. Res.*, IAHR 39(2), 203–209. Discussion: (2002). 40(3), 379–384.

[42] Ippen, A.T., Kulin, G. (1957). The effect of boundary resistance on solitary waves. *Houille Blanche*, 12(3), 390–400.

[43] Dingemans, M.W. (1997). Water wave propagation over uneven bottoms. Advanced series on ocean engineering, Vol. 13, World Scientific, Singapore.

[44] Nielsen, P. (2009). Coastal and estuarine processes, World Scientific, Singapore.

[45] Gualtieri, C., and Chanson, H. (2011). "Experimental Study of a Positive Surge. Part 2: Comparison with Literature Theories and Unsteady Flow Field Analysis." *Environmental Fluid Mechanics*, 11(6), pp.641-651 (DOI 10.1007/s10652-011-9222-3).